CLINICAL ORAL IMPLANTS RESEARCH

Carlo Maria Soardi
Emanuele Clozza
Gianluca Turco
Matteo Biasotto
Steven P. Engebretson
Hom-Lay Wang
Davide Zaffe

Microradiography and microcomputed tomography comparative analysis in human bone cores harvested after maxillary sinus augmentation: a pilot study

Authors' affiliations:
Carlo Maria Soardi, Private Practice, Brescia, Italy
Emanuele Clozza, Steven P. Engebretson, Department of Periodontology and Implant Dentistry, New York University College of Dentistry, New York, NY, USA
Gianluca Turco, Matteo Biasotto, Department of Medical Sciences, University of Trieste, Trieste, Italy
Hom-Lay Wang, Department of Periodontics and Oral Medicine, School of Dentistry, University of Michigan, Ann Arbor, MI, USA
Davide Zaffe, Department of Biomedical, Metabolic and Neural Sciences, University of Modena and Reggio Emilia, Modena, Italy

Corresponding author:
Dr. Emanuele Clozza
Ashman Department of Periodontology and Implant Dentistry
New York University College of Dentistry
345 East 24th Street, Suite 3W, New York, NY 10010, USA
Tel.: +1(212)992 7040
Fax: +1(212)995 3961
e-mail: leleclo@libero.it

Key words: bone formation, bone graft, bone histomorphometry, microcomputed tomography, microradiography

Abstract

Objectives: The aim of this study was to compare microradiography (MR) and microcomputed tomography (μCT) analysis of bone samples following maxillary sinus augmentation at different time periods and determine the relationships between measured area and volume fractions.

Materials and methods: Lateral window sinus grafts were performed on 10 patients using a mineralized human bone allograft (MHBA). At implant placement, 5–13 months after surgery, 10 bone core biopsies were harvested. Prior to histologic sectioning, bone samples were evaluated with μCT. The morphometric parameters computed by MR and μCT were compared using Pearson's correlation and Bland and Altman analysis and included hard tissue fraction (HV/TV:%), soft tissue fraction (SV/TV:%), vital bone fraction (BV/TV:%) and residual graft fraction (GV/TV:%).

Results: Strong positive correlation between MR and μCT was found for HV/TV and SV/TV and BV/TV [r = 0.84, 0.84 and 0.69, respectively] but weak for GV/TV [r = 0.10].

Conclusion: μCT technology shows promising potential as an indicator of bone morphology changes; however, caution should be used in interpreting morphometric parameters, as the different methods reveal important biases.

Date:
Accepted 3 June 2013

To cite this article:
Soardi CM, Clozza E, Turco G, Biasotto M, Engebretson SP, Wang H-L, Zaffe D. Microradiography and microcomputed tomography comparative analysis in human bone cores harvested after maxillary sinus augmentation: a pilot study. *Clin. Oral Impl. Res.* **25**, 2014, 1161–1168
doi: 10.1111/clr.12225

The human maxillary sinus is one of the most intensely studied anatomic regions with regard to placing dental implants. Systematic reviews suggest that the survival rate of implants placed into augmented sinuses is the same as that of placed in native bone of maxillary posterior areas (Wallace & Froum 2003; Del Fabbro et al. 2004; Aghaloo & Moy 2007; Chiapasco et al. 2009). Regardless of the material used for augmentation, the structure of the graft after healing must provide a microarchitecture that allows a sufficient implant anchorage through osseointegration (Kühl et al. 2010). Traditionally, bone histomorphometry has been employed to evaluate the trabecular architecture by extrapolating two-dimensional (2D) measurements to three-dimensional (3D) space (Parfitt et al. 1987). A limitation of this method is that the samples are destroyed in the process, preventing the specimens from being used for other assessments (Yeom et al. 2008). Moreover, the distribution of cancellous bone is heterogeneous, and bone histomorphometry analysis is restricted to only 2D fields of view (Bonnet et al. 2009).

Recently, microcomputed tomography (μCT) system has attracted increasing attention in bone tissue engineering as a powerful non-destructive diagnostic tool that allows exploring the microstructure in a 3D manner. μCT has been used in several recent human studies to quantify newly formed bone and residual graft material in human biopsy specimens sampled after sinus floor elevation (Trisi et al. 2006; Stiller et al. 2009; Chackartchi et al. 2010; Chappard et al. 2010; Kühl et al. 2010, 2013; Caubet et al. 2011; Emam et al. 2011; Huang et al. 2011).

Because μCT is a relatively new technique, the procedures and application utilized to elucidate the integration of bone regeneration materials in 3D bone architecture are not yet fully standardized (Stiller et al. 2009). To establish μCT as a method for evaluation of the remodeling of biomaterials after grafting

procedure, the method has to be validated by evaluating a certain number of bone biopsy specimens and comparing those results to the gold standard which remains histological imaging.

In a previous study, conventional histology was used to examine the effect of mineralized human bone allograft (MHBA) on bone formation at 6 and 9 months after sinus floor augmentation (Soardi et al. 2011). Microradiography (MR) was used to determined histomorphometrically bone area fractions and residual graft area fractions in each biopsy specimen. MR is an imaging technique using X-rays that provides a high-resolution picture of a histologic section. It is commonly utilized to measure mineral distributions (calcium, phosphate) and mineral amounts of carious lesions in enamel and dentin (Josselin et al. 1997). The technique has shown to detect bony boundaries with accuracy (Schortinghuis et al. 2003). However, the inherent limitation of this method is that the evaluation of regenerated bone and residual graft volume was based on 2D measurements of a selected area within the sample. Therefore, we hypothesized that analysis of the entire sample by μCT might reveal new information concerning new bone and residual graft volume. Although several studies have compared results obtained by histomorphometry and μCT in relation to bone specimens (Ito et al. 1998; Müller et al. 1998; Laib & Ruegsegger 1999; Chappard et al. 2005; Hedberg et al. 2005; Gielkens et al. 2008; González-García & Monje 2012a,b;) and in assessing osseointegration and bone formation around implants (Park et al. 2005; Liu et al. 2011; Bernhardt et al. 2012,), no human studies have validated the μCT quantification of regenerated bone following grafting procedure. The present study aimed to compare MR with μCT of bone cores harvested from regenerated maxillary sinuses after different periods of healing and determine the relationships between measured area and volume fractions.

Materials and methods

Study design

Ten patients (three women and seven men, between 27 and 71 years of age) were selected from a pool of subjects requiring maxillary sinus augmentation for the placement of delayed posterior implants. All patients were partially or totally edentulous and in need of unilateral maxillary sinus augmentation. The recruitment and active treatment period was October 2010–November 2011 and carried out by the same operator (C.M.S) in a private dental office in Brescia, Italy. Patients were systemically healthy; they did not smoke nor take any medications. Additional inclusion criteria were absence of sinus disease and <1 mm of crestal bone height of the sinus floor, as measured on the serial section of the CT scan.

The study was conducted following the ethical principles founded in the Declaration of Helsinki (Puri et al. 2009); a written consent form was obtained from all eligible patients.

Surgical procedures

A pre-operative panoramic radiograph and a CT scan (at increasing depth of 1 mm intervals) of the maxilla were taken for each patient. The width of the sinus was evaluated in the CT section corresponding to the position where the implant was to be inserted based on the prosthetic treatment plan. The sagittal CT section was identified using a diagnostic template, coated with radiopaque material. The distance between the palatal and buccal wall was measured 10 mm cranially to the residual bone crest using a radiographic software (3 Diagnosis 3.0, 3DIEMME S.r.l., Cantù, Como, Italy) in order to place sufficient bone graft material to accommodate at least a 10 mm implant.

Maxillary sinus augmentation and postoperative care were performed as described in a previous publication (Soardi et al. 2011).

Five to 13 months after sinus augmentation procedures, patients returned for implant surgery. At the time of surgery, local infiltration of anesthetic with an epinephrine concentration of 1 : 100,000 was administered (Ultracain 3DIEMME D-S, Sanofi-Aventis Deutschland GmbH, Frankfurt am Main, Germany). A full-thickness crestal incision was made slightly toward the palate, and a buccal full-thickness flap was reflected to

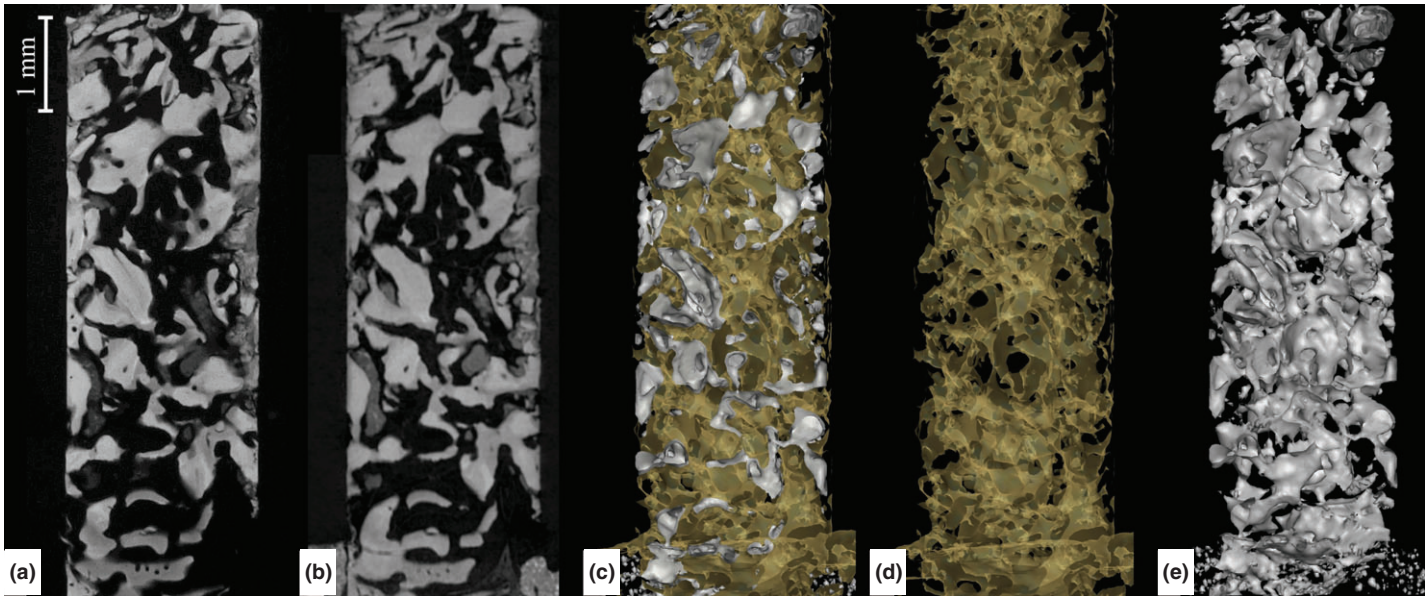

Fig. 1. Representative image showing the labeling method for μCT quantification. (a) MR of a histologic section of bone sample of maxillary sinus floor augmented by MHBA 5 months after healing. (b) The corresponding μCT slice in gray-scales of the by a manual scanning procedure. (c) 3D visualization of the corresponding μCT slice: hard tissue phase represented by yellow surfaces and residual graft by white surfaces, (d) vital bone phase represented by yellow surfaces and (e) residual graft phase represented by white surfaces.

expose the residual bone crest. A trephine drill with external diameter of 4 mm and internal diameter of 3 mm (Stroma GmbH, Emmingen-Liptingen, Germany), under a saline irrigation at 600 rpm, was utilized (up to 10 mm) to collect bone core specimens before implant insertion (Tapered Screw Vent, Zimmer Dental Inc., Carlsbad, CA, USA). A total of 10 osseointegrated implants were placed, one in each patient. The bone core specimens were collected with the assistance of surgical guides that were based upon the individual prosthetic requirements. Retrieved bone core samples were marked on their crestal aspects and immediately fixed in 4% paraformaldehyde (Fluka, Sigma-Aldrich Schweiz, Buchs SG, Switzerland) in 0.1 M phosphate buffer pH 7.2 for 4 h at room temperature. Samples were washed with the buffer and dehydrated through an ethanol series.

μCT

Bone samples were examined by one operator (G.T.) with a μCT machine called TOMOLAB (ELETTRA Synchrotron Light Laboratory, Trieste, Italy). The device was equipped with a sealed microfocus tube, which guaranteed an X-ray energy range of 40 kV and a current of 200 μA. As a detector, a CCD digital camera was used with a 49.9 × 33.2 mm^2 field of view and a pixel size of 12.5 × 12.5 μm^2. The samples were positioned onto the turn-table of the instrument, and acquisitions were performed with the following parameters: distance source-sample (FOD), 100 mm; distance source-detector (FDD), 400 mm; magnification, 4 ×; binning, 2 × 2; resolution of 8.33 μm in all three dimensions; tomographies dimensions of 1984 × 1984 × 1024 pixels; and slices dimensions of 265 × 265 (range of slices from 465 to 1149). The slices reconstruction process achieved by means of commercial software (Cobra Exxim, Pleasanton, CA, USA) started once the tomographic scan was completed, and all the projections were transferred to the workstation. Input projections and output slices were represented by files (one file per projection and one file per slice) using arrays of 16-bit integers.

Microradiography

After μCT analysis, the cylindrical bone samples were dehydrated and embedded in polymethyl methacrylate (PMMA) using a water bath at 4°C as described elsewhere (Bertoldi et al. 2008). Each PMMA block was serially sectioned along the longitudinal axis of the cylindrical bone samples to their center using a diamond saw microtome (SP1600, Leica Micro-system, Wetzlar, Germany). A thick section (200 mm) was obtained from the center of the bone cores using the diamond saw microtome. Each section was reduced to 100 mm by grinding, perfectly polished with emery paper and alumina, and then microradiographed (3K5, Italstructures, Riva del Garda, Trento, Italy) at 15 kV and 10 mA on high-resolution film (SO 343, Eastman Kodak Co., Rochester, NY, USA). The MRs and the sections were analyzed and photographed by the same operator (D.Z.) using a microscope (Axiophot, Carl Zeiss AG, Oberkochen, Germany) under ordinary light. The amount of total tissue (TV: mm^2), hard tissue (HV: mm^2), soft tissue (SV: mm^2), vital bone (BV: mm^2), residual graft (GV: mm^2) and hard tissue surface (HS: mm) was measured on the MRs using a program for image analyzer and software (AnalySIS, Soft Imaging System GmbH, Münster, Germany). Then, the following amounts of tissue components were obtained: hard tissue fraction (HV/TV:%), soft tissue fraction (SV/TV:%), vital bone fraction (BV/TV:%) and residual graft fraction (GV/TV:%).

Visualization and analysis procedures for μCT quantification

The complete μCT data set was loaded into a workstation and evaluated with Amira (version 5.5.2, Mercury computer Systems, Chelmsford, MA, USA) by the same operator (E.C.). The first step was to separate the object from the background: this was done by select-

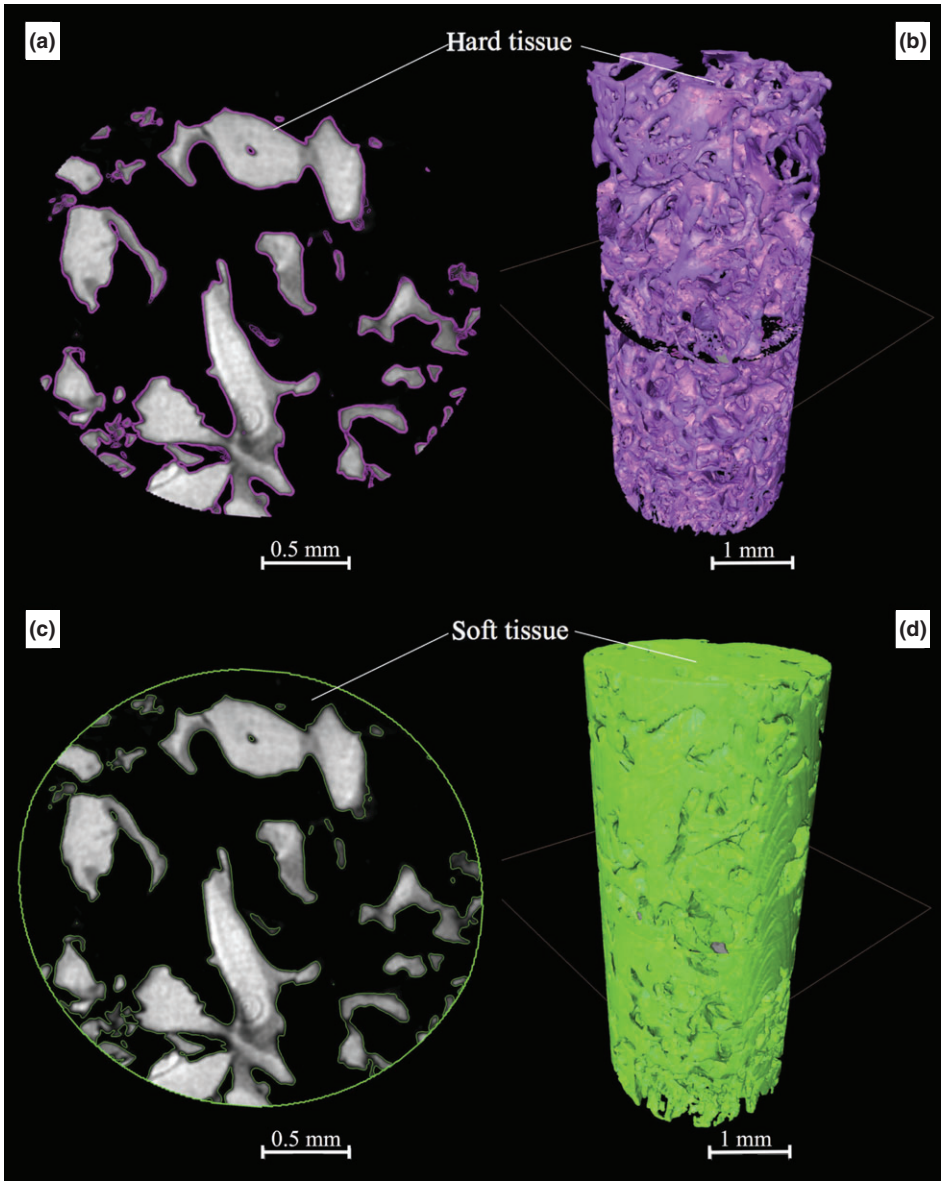

Fig. 2. Hard and soft tissue segmentation: (a-c) slices in gray-scales and (b-d) 3D visualization of the corresponding tissue.

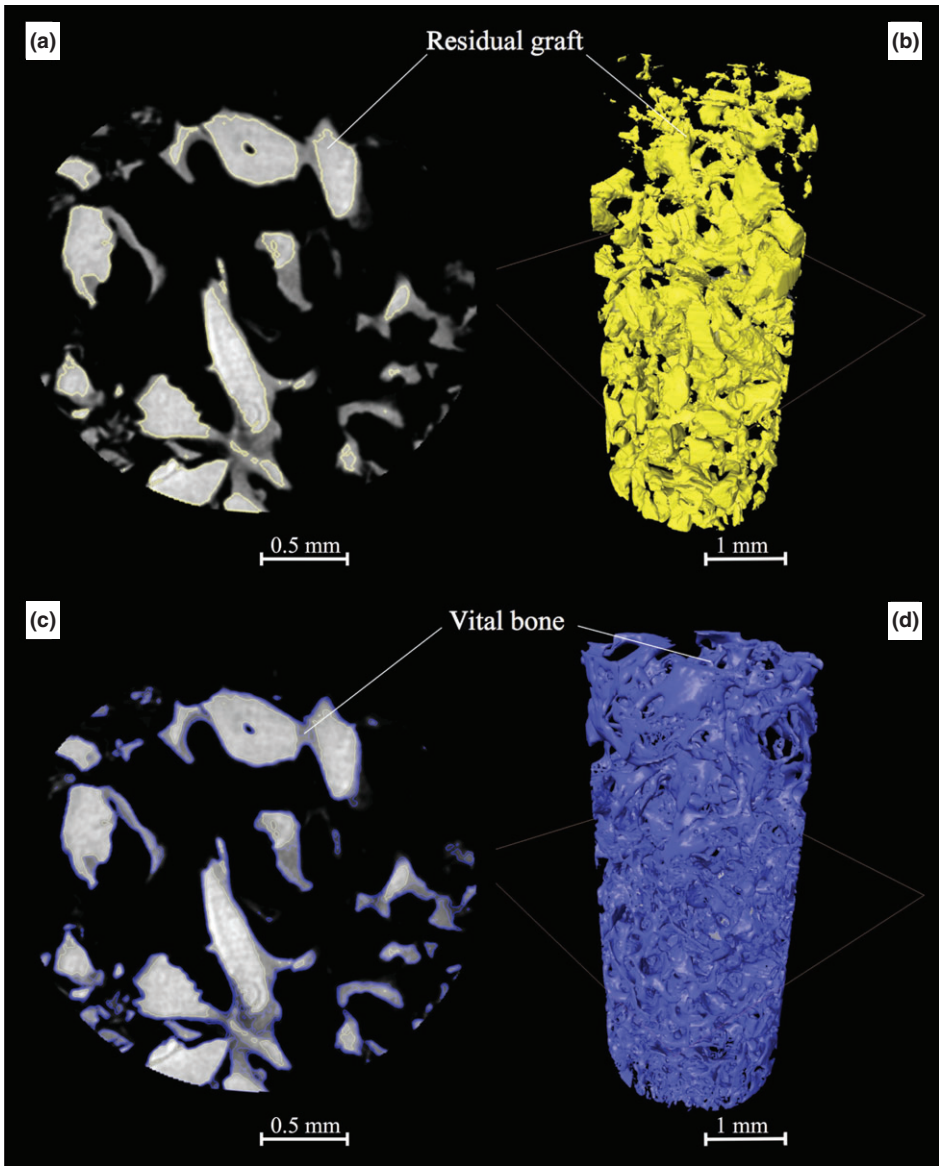

Fig. 3. Residual graft and vital bone segmentation: (a-c) slices in gray-scales and (b-d) 3D visualization of the corresponding tissue

Table 1. **Descriptive statistics of data obtained with the two applied methods**

n = 10; 5–13 months after healing Morphometric parameters	Mean	Median	SD	Min	Max
μCT HV/TV (%)	56.96	56.84	13.03	31.04	77.17
MR HV/TV (%)	49.73	50.53	8.08	33.11	59.64
μCT SV/TV (%)	43.04	49.47	13.74	22.83	68.96
MR SV/TV (%)	50.27	49.47	8.08	40.36	66.89
μCT BV/TV (%)	37.2	34.65	13.41	17.82	57.92
MR BV/TV (%)	27.8	20.24	8.4	20.24	42.86
μCT GV/TV (%)	19.55	17.58	6.35	12.87	34.77
MR GV/TV (%)	21.95	19.47	7.99	11.52	35.57

ing a cylindrical volume of interest (VOI) with the dimension of the bone sample in the virtual image data. This VOI excluded voxels outside this region and replaced them by the zero level port. The gray value image stacks acquired from the μCT were examined section by section. Then, the tissue structures of interest were manually labeled with the "*segmentation editor*" tool in Amira, at best visual agreement with the histologic information (Fig. 1). In this process, any group of voxels belonging to a particular tissue structure was given a unique label resulting in a stack of label images corresponding to the underlying μCT images. Four different kinds of tissues were recognized: hard tissue (the mineralized part of the sample, which included the vital bone and residual graft), vital bone, soft tissue (the unmineralized part of the sample) and residual graft (Figs. 2a-c and 3a-c). These label images were subsequently used to reconstruct polygonal surface models (Figs. 2b-d. and 3b-d**).** The *"MaterialStatistics"* tool in Amira quantified the surface and volume of each labeled structure. From these measures, the total amount of tissue (TV: mm^3), hard tissue (HV: mm^3), soft tissue (SV: mm^3), vital bone (BV: mm^3), residual graft (GV: mm^3) and hard tissue surface (HS: mm^2) were calculated. To be able to compare samples with different sizes, the normalized indices HV/TV (%), BS/TV (mm^{-1}), BV/TV (%) and GV/TV (%) were used.

Statistical analysis

Descriptive statistics were used to present data obtained by the two different methods. A Mann–Whitney *U*-test and Pearson's correlation analysis were then performed; $P < 0.05$ was considered statistically significant. To assess the degree of agreement between MR and μCT, we compared the results using the analysis of Bland & Altman (1986), as previously used by Gielkens et al. 2008 and Yeom et al. (2008). The statistical analyses were performed using SPSS 19.0 for Windows (SSPS, Inc., Chicago, IL, USA) and XLSTAT 2012.4.01 for Mac OS (Addinsoft, Paris, France).

Results

Clinical findings

Primary wound closure was observed after the first and the second operations (sinus augmentation and implant placement surgery) and during the follow-up. All the 10 implants healed submerged without any exposure. Five to thirteen months after sinus augmentation procedures, all patients had sufficient bone levels for the placement of the implants and with adequate primary stability. No implant failures were noted up to the time of the completion of this manuscript (1 year after implant surgery). Biopsies varied in length between patients.

Microradiography

The descriptive statistics of the MR tissue percentages are shown in Table 1. Five to thirteen months after healing, the biopsies showed a composite formed by MHBA particles and

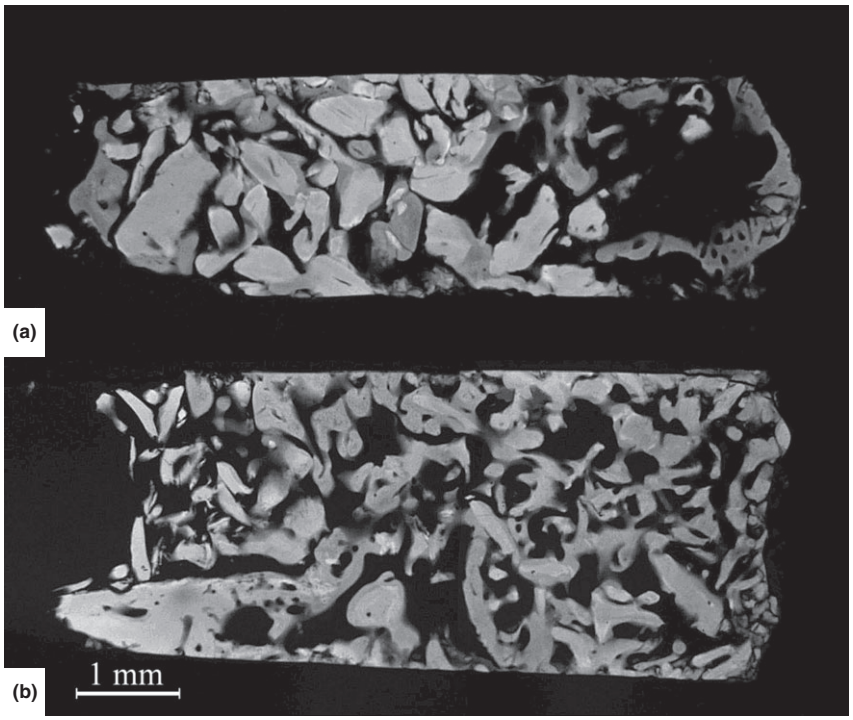

Fig. 4. Representative image showing two MRs of a histologic section of bone samples of maxillary sinus floor augmented by MHBA, 7 (a) and 10 (b) months after healing. Note in (a) the bone apposition occurring on the surface of the residual particles. A network of newly formed bony trabeculae and scaffold degradation is shown in (b).

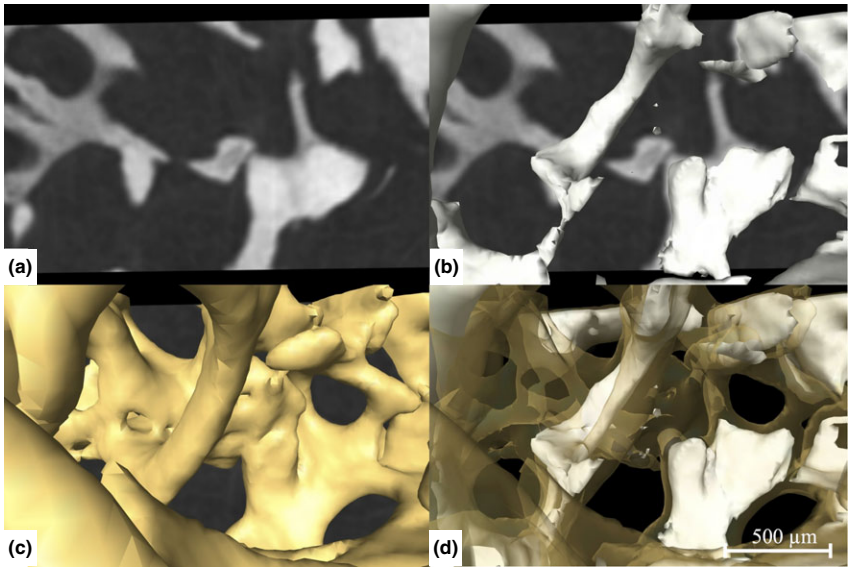

Fig. 5. μCT of bone sample harvested 6 months following maxillary sinus augmentation. (a) μCT slice in grayscales. (b) 3D visualization of the corresponding μCT slice: residual graft phase represented by white surfaces (c) vital bone phase represented by yellow surfaces and (d) hard tissue phase represented by both yellow and white surfaces.

Table 2. **Relationships between data compared with Pearson's correlation and Bland and Altman analysis. Biases are expressed as percentages of the values on the axis**

n = 10; 5–13 months after healing Morphometric parameters	μCT vs. MR *r* (%)	*p-value*	Bias (%) [95% CI]
HV/TV	0.84	0.218	11.88 [1.86, 21.90]
SV/TV	0.84	0.218	−18.90 [−34.79, −3.00]
BV/TV	0.69	0.218	25.11 [0.71, 49.52]
GV/TV	0.10	0.579	−9.97 [−38.26, 18.31]

newly formed trabecular bone. The majority of MHBA particles directly connected with the newly formed bone whereas very few ones surrounded by the fibrous tissue (Figs. 4a,b).

μCT

The descriptive statistics of the μCT tissue percentages are shown in Table 1. In all bone biopsies samples, MHBA residual particles were identified in the μCT slices due to their higher gray values when compared with bone (Fig. 5a) and easily reconstructed in a 3D manner (Fig. 5b). Newly formed *trabeculae* were noted with typical aspect of the tissue with woven structure (Fig. 5c). The bone completely surrounded the residual graft (Fig. 5d).

Correlation and agreement of histomorphometry and μCT

A summary of statistical results of Pearson's correlation and Bland and Altman analysis is presented in Table 2 and in Fig. 6.

Discussion

Bone quality depends on the structural and material properties of bone, which include its microarchitecture (Felsenberg & Boonen 2005). Many clinical studies have established the direct correlation between bone quality and implant success rates (Cox & Zarb 1987; Engquist et al. 1988). Studies evaluating new bone substitutes by μCT employ morphometric parameters to assess bone microarchitecture in regenerated implant sites. The aim of this pilot study was to compare a 2D semiquantitative analysis obtained by MR with a 3D quantitative analysis assessed by μCT. In particular, we studied the correlation and agreement by comparing morphometric parameters traditionally used in bone histomorphometry that were calculated from both MR sections and the μCT entire data volume. The current histomorphometric data of BV/TV and GV/TV were in agreement with that published recently (Soardi et al. 2011). When evaluating the microstructure of bone samples, MR and μCT differ greatly according to morphometric parameter measured. In fact, although strong correlation was found for HV/TV, SV/TV and BV/TV (r = 0.84, 0.84 and 0.69, respectively), weak association existed for GV/TV (r = 0.10).

The correlation between bone histomorphometry and μCT with regards to bone volume fraction remains contradictory in literature. Some studies have shown high correlation

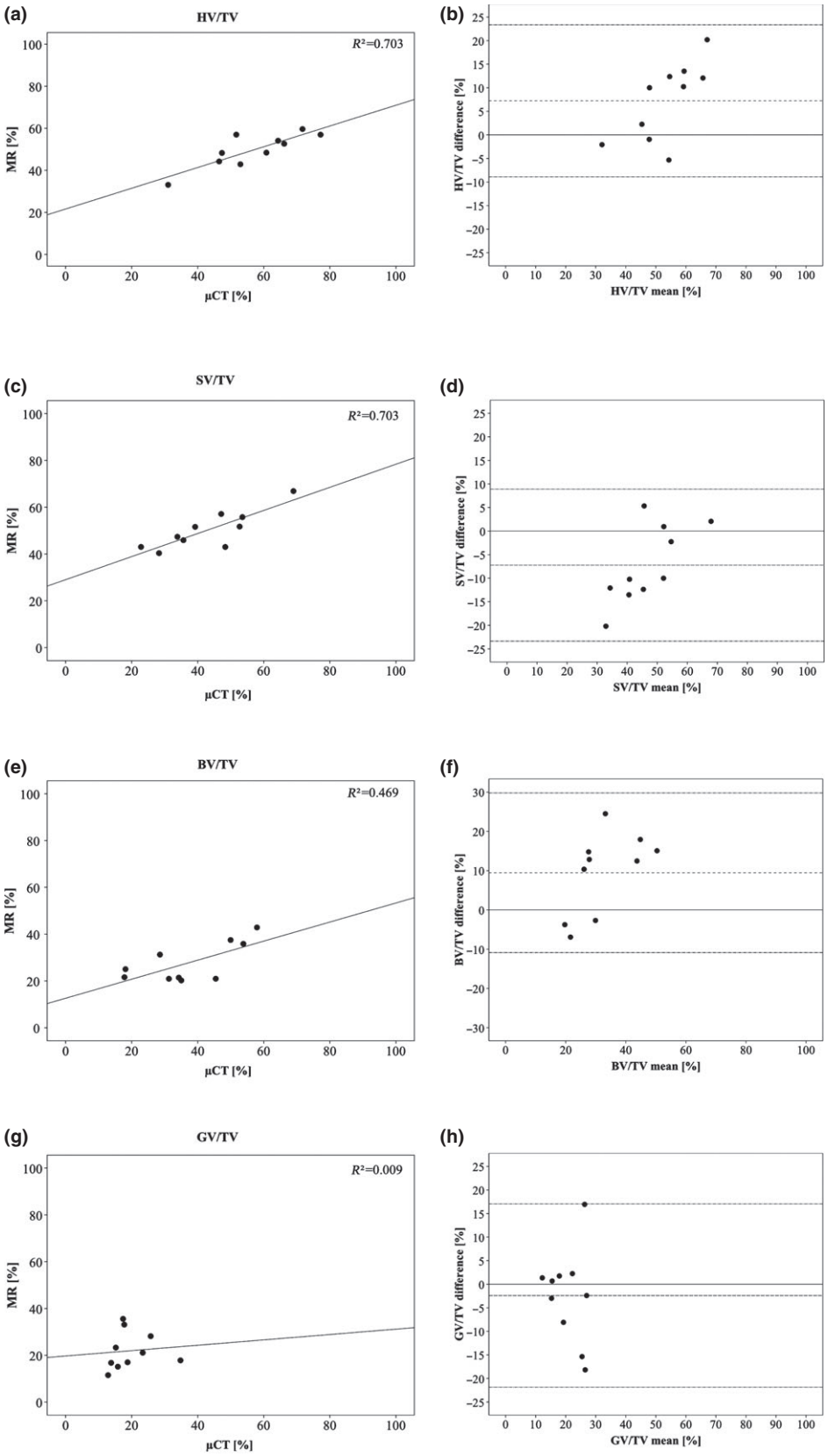

Fig. 6. (a, c, e and g) Relationships between MR and _CT used for measuring the HV/TV, SV/TV, BV/TV and GV/TV with the line of equity (solid line). (b, d, f and h) The graphs display a scatter diagram of the differences of the values plotted against the averages of the two applied methods. Horizontal lines are drawn at the zero value (solid line), at mean difference describing the bias between the applied methods (dot-dashed line) and at the limits of agreement (dashed lines) which are defined as the mean difference plus and minus 1.96 times the standard deviation of the differences.

between hard tissue fraction values obtained from histologic sections and μCT data sets (Uchiyama et al. 1997; Müller et al. 1998; Cendre et al. 1999; Banse et al. 2002; Chappard et al. 2005; Thomsen et al. 2005)—and the result of our study is not that far from the previously reported findings—while other studies revealed moderate correlation (Ito et al. 1998; Tamminen et al. 2010).

Stiller et al. (2009) compared the validity of histomorphometry to 2D slice and 3D entire data volume obtained by synchrotron μCT (SRμCT) from two bone biopsies harvested after maxillary sinus elevation. A good agreement between both methods was achieved in assessing the bone area fraction, with only a minor difference of 1.6%. In the present study, we found an acceptable degree of agreement between methods, with overestimation of HV/TV (+11.88%) and BV/TV (+25.11%) and an underestimation of SV/TV (−18.90%). It seems reasonable that these major differences could be related mainly to the greater number of samples utilized in the present study.

The Bland and Altman plots revealed a skewed distribution. In particular, the differences tended to be negative when the tissue percentage was low, whereas positive when it was high.

Although the discrepancy between the applied methods to measure GV/TV was relatively small, a non-significant weak positive correlation was found, indicating no predicable relationship regarding this parameter.

An explanation for this inconsistency could have methodical based reasons: in both methods, it was complex to automatically distinguish the exact borders between the vital bone and MHBA particles, specifically in those samples where the maturation phase had reached an advanced stage in which the radiolucency of the residual graft appeared to be similar to the newly formed bone. This phenomenon has been described before. For instance, Schmitt et al. (2013) performed a clinical investigation by comparing different bone substitutes using MR and histology, and they could not perform the quantification of MHBA particles due to the similarity in appearance of the transplant and the newly formed bone. Likewise, Chackartchi et al. (2010) reported that it was difficult to distinguish in the μCT image the exact borders between the new bone and graft particles.

Chappard et al. (2005) pointed out that the ratios of quantities expressed as a percentage were more comparable between studies. They showed that parameters reported in a given unit could have suffered large variations

because bone surface appeared to have a fractal dimension under some limits. Furthermore, measurements could have been modified by various factors, which included the magnification, the structural elements used by the software for calculations and the different maturation status of the bone samples.

Additional factors contributing to the quality of the quantitative μCT assessment are the system resolution and the effect of the segmentation on the morphometric parameters. Although μCT slices have high resolution (8.33 μm in all three dimensions) and a *quasi*-histological appearance, the 3D quantification performed with AMIRA showed important disagreements when compared with MR measurements. These biases may have originated also for the process of obtaining threshold values during their calculation. Ding and coworkers demonstrated that attention must be taken when applying thresholds in generating 3D data sets, if one is interested in an accurate investigation of trabecular bone microstructure (Feldkamp et al. 1989).

Müller et al. (1998) argued that the individualized threshold determination would make quantitative analysis very difficult, and the use of a uniform threshold was an adequate procedure for the evaluation and differentiation of both normal and osteoporotic human iliac bone. In our present experiment, we used an adaptive threshold to account for the possible variations in density levels. It should be noted that not only for different specimens, but even within samples, a uniform threshold approach is inappropriate for μCT measurements (Ding et al. 1999; Ding & Hvid 2000).

Scherf & Tilgner (2009) observed that gray value variations in trabecular bone were an important source of error in single threshold segmentation as the results of single thresholding segmentation methods depend on the attenuation properties of trabecular bone. For instance, if the majority of the bone has relatively high gray values, the threshold will be inappropriately high for those areas with low gray values and parts of these structures will be disregarded in the segmentation. In contrast, regions with high gray values will be enlarged when the majority of the bone has lower gray values.

Our study is limited by the relatively low number of biopsies ($n = 10$). However, significant differences between the groups were revealed for the majority of the morphometric parameters considered in the experiment. A greater number of bone biopsy specimens for gathering the required volume information are necessary to verify whether our findings are consistent. μCT may not be applicable routinely in clinical practice for now; this limitation creates a need to find a relationship between this method and other ones accessible to clinicians. Among the pre-operative diagnostic tools to characterize bone quality, cone beam computed tomography (CBCT) grey levels have shown good correlation ($r = 0.77$) with histomorphometric bone density values assessed by MR (Soardi et al. 2012).

In our study, only the central slice sectioned along the longitudinal axis of the cylindrical bone sample was utilized to assess morphometric parameters. Bernhardt et al. (2012) compared the results of bone–implant contact (BIC) obtained by histological sections and SRμCT. The authors illustrated the fact that the selection of histologic section may strongly influence the determined BIC and that at least 3–4 histological sections are necessary to represent the BIC for a sample. Hence, future studies should investigate whether multiple sections analyzed histomorphometrically and compared with the μCT entire volume data may improve correlation and agreement of these morphometric measurements.

Finally, one must keep in mind that certain biological events cannot be observed by μCT, for example cell alignment, cell shape, localization of proteins or enzyme detection. Therefore, the biological information obtained by histology should never be neglected.

Conclusions

In conclusion, the present study suggests that when evaluating micro-architecture to assess bone quality in regenerated implant sites at different maturation phases, the correlation and agreement between MR and μCT varies according to the morphometric parameter measured. μCT technology shows promising potential as an indicator of bone morphology changes; however, caution should be used in interpreting morphometric parameters, as the different methods reveal important biases.

Acknowledgements: The authors declare that they have no conflict of interests. The study was self-supported.

References:

Aghaloo, T.L. & Moy, P.K. (2007) Which hard tissue augmentation techniques are the most successful in furnishing bony support for implant placement? *The International Journal of Oral Maxillofacial Implants* **22** Suppl: 49–70.

Banse, X., Devogelaer, J.P. & Grynpas, M. (2002) Patient-specific microarchitecture of vertebral cancellous bone: a peripheral quantitative computed tomographic and histological study. *Bone* **30**: 829–835.

Bernhardt, R., Kuhlisch, E., Schulz, M.C., Eckelt, U. & Stadlinger, B. (2012) Comparison of bone-implant contact and bone-implant volume between 2D-histological sections and 3D-SRμCT slices. *European Cells & Materials* **23**: 237–248.

Bertoldi, C., Zaffe, D. & Consolo, U. (2008) Polylactide/polyglycolide copolymer in bone defect healing in humans. *Biomaterials* **29**: 1817–1823.

Bland, J.M. & Altman, D.G. (1986) Statistical methods for assessing agreement between two methods of clinical measurement. *Lancet* **1**: 307–310.

Bonnet, N., Laroche, N., Vico, L., Dolleans, E., Courteix, D. & Benhamou, C.L. (2009) Assessment of trabecular bone microarchitecture by two different x-ray microcomputed tomographs: a comparative study of the rat distal tibia using Skyscan and Scanco devices. *Medical Physics* **36**: 1286–1297.

Caubet, J., Petzold, C., Sáez-Torres, C., Morey, M., Iriarte, J.I., Sánchez, J., Torres, J.J., Ramis, J.M. & Monjo, M. (2011) Sinus graft with safescraper: 5-year results. *Journal of Oral Maxillofacial Surgery* **69**: 482–490.

Cendre, E., Mitton, D., Roux, J.P., Arlot, M.E., Duboeuf, F., Burt-Pichat, B., Rumelhart, C., Peix, G. & Meunier, P.J. (1999) High-resolution computed tomography for architectural characterization of human lumbar cancellous bone: relationships with histomorphometry and biomechanics. *Osteoporosis International* **10**: 353–360.

Chackartchi, T., Iezzi, G., Goldstein, M., Klinger, A., Soskolne, A., Piattelli, A. & Shapira, L. (2010) Sinus floor augmentation using large (1-2 mm) or small (0.25-1 mm) bovine bone mineral particles: a prospective, intra-individual controlled clinical, micro-computerized tomography and histomorphometric study. *Clinical Oral Implants Research* **22**: 473–480.

Chappard, D., Guillaume, B., Mallet, R., Pascaretti-Grizon, F., Baslé, M.F. & Libouban, H.L.N. (2010) Sinus lift augmentation and beta-TCP: a microCT and histologic analysis on human bone biopsies. *Micron* **41**: 321–326.

Chappard, D., Retailleau-Gaborit, N., Legrand, E., Baslé, M.F. & Audran, M. (2005) Comparison insight bone measurements by histomorphometry and μCT. *Journal of Bone and Mineral Research* **20**: 1177–1184.

Chiapasco, M., Casentini, P. & Zaniboni, M. (2009) Bone augmentation procedures in implant dentistry. *The International Journal of Oral Maxillofacial Implants* **24** Suppl: 237–259.

Cox, J.F. & Zarb, G.A. (1987) The longitudinal clinical efficacy of osseointegrated dental implants: a 3-year report. *The International Journal of Oral Maxillofacial Implants* **2**: 91–100.

Del Fabbro, M., Testori, T., Francetti, L. & Weinstein, R. (2004) Systematic review of survival rates for implants placed in the grafted maxillary sinus. *The International Journal of Periodontics and Restorative Dentistry* **24**: 565–577.

Ding, M. & Hvid, I. (2000) Quantification of age-related changes in the structure model type and trabecular thickness of human tibial cancellous bone. *Bone* **26**: 291–295.

Ding, M., Odgaard, A. & Hvid, I. (1999) Accuracy of cancellous bone volume fraction measured by micro-CT scanning. *Journal of Biomechanics* **32**: 323–326.

Emam, H., Beheiri, G., Elsalanty, M. & Sharawy, M. (2011) Microcomputed tomographic and histologic analysis of anorganic bone matrix coupled with cell-binding peptide suspended in sodium hyaluronate carrier after sinus augmentation: a clinical study. *The International Journal of Oral Maxillofacial Implants* **26**: 561–570.

Engquist, B., Bergendal, T. & Kallus, T. (1988) A retrospective multicenter evaluation of osseointegrated implants supporting overdentures. *The International Journal of Oral Maxillofacial Implants* **3**: 129–134.

Feldkamp, L.A., Goldstein, S.A., Parfitt, A.M., Jesion, G. & Kleerekoper, M. (1989) The direct examination of three-dimensional bone architecture in vitro by computed tomography. *Journal of Bone and Mineral Research* **4**: 3–11.

Felsenberg, D. & Boonen, S. (2005) The bone quality framework: determinants of bone strength and their interrelationships, and implications for osteoporosis management. *Clinical Therapy* **27**: 1–11.

Gielkens, P.F., Schortinghuis, J., de Jong, J.R., Huysmans, M.C., Leeuwen, M.B., Raghoebar, G.M., Bos, R.R. & Stegenga, B. (2008) A comparison of micro-CT, microradiography and histomorphometry in bone research. *Archives of Oral Biology* **53**: 558–566.

González-García, R. & Monje, F. (2012a) The reliability of cone-beam computed tomography to assess bone density at dental implant recipient sites: a histomorphometric analysis by micro-CT. *Clinical Oral Implants Research* doi: 10.1111/j.1600-0501.2011.02390.x. [Epub ahead of print].

González-García, R. & Monje, F. (2012b) Is microcomputed tomography reliable to determine the microstructure of the maxillary alveolar bone? *Clinical Oral Implants Research* **2012**: doi:10.1111/j.1600-0501.2012.02478.x.

Hedberg, E.L., Kroese-Deutman, H.C., Shih, C.K., Lemoine, J.J., Liebschner, M.A., Miller, M.J., Yasko, A.W., Crowther, R.S., Carney, D.H., Mikos, A.G. & Jansen, J.A. (2005) Methods: a comparative analysis of radiography, microcomputed tomography, and histology for bone tissue engineering. *Tissue Engineering* **11**: 1356–1367.

Huang, H.-L., Chen, M.Y., Hsu, J.-T., Li, Y.-F., Chang, C.-H. & Chen, K.-T. (2011) Three-dimensional bone structure and bone mineral density evaluations of autogenous bone graft after sinus augmentation: a microcomputed tomography analysis. *Clinical Oral Implants Research* **23**: 1098–1103.

Ito, M., Nakamura, T., Matsumoto, T., Tsurusaki, K. & Hayashi, K. (1998) Analysis of trabecular microarchitecture of human iliac bone using microcomputed tomography in patients with hip arthrosis with or without vertebral fracture. *Bone* **23**: 163–169.

Josselin, De, de Jong, J.E., ten Bosch, J.J. & Noordmans, J. (1997) Optimised microcomputer-guided quantitative microradiography on dental mineralised tissue slices. *Physics in Medicine & Biology* **32**: 887–899.

Kühl, S., Brochhausen, C., Götz, H., Filippi, A., Payer, M., d'Hoedt, B. & Kreisler, M. (2013) The influence of bone substitute materials on the bone volume after maxillary sinus augmentation: a microcomputerized tomography study. *Clinical Oral Investigations* **17**: 543–551.

Kühl, S., Götz, H., Hansen, T., Kreisler, M., Behneke, A., Heil, U., Duschner, H. & d'Hoedt, B. (2010) Three-dimensional analysis of bone formation after maxillary sinus augmentation by means of microcomputed tomography: a pilot study. *The International Journal of Oral Maxillofacial Implants* **25**: 930–938.

Laib, A. & Ruegsegger, P. (1999) Calibration of trabecular bone structure measurements of *in vivo* three-dimensional peripheral quantitative computed tomography with 28-micron-resolution microcomputed tomography. *Bone* **24**: 35–39.

Liu, S., Broucek, J., Virdi, A.S. & Sumner, D.R. (2011) Limitations of using micro-computed tomography to predict bone-implant contact and mechanical fixation. *Journal of Microscopy* **245**: 34–42.

Müller, R., Van Campenhout, H., Van Damme, B., Van Der Perre, G., Dequeker, J., Hildebrand, T. & Rüegsegger, P. (1998) Morphometric analysis of human bone biopsies: a quantitative structural comparison of histological sections and micro-computed tomography. *Bone* **23**: 59–66.

Parfitt, A.M., Drezner, M.K., Glorieux, F.H., Kanis, J.A., Malluche, H., Meunier, P.J., Ott, S.M. & Recker, R.R. (1987) Bone histomorphometry: standardization of nomenclature, symbols, and units. report of the ASBMR histomorphometry nomenclature committee. *Journal of Bone Mineral Research* **2**: 595–610.

Park, Y.-S., Yi, K.-Y., Lee, I.-S. & Jung, Y.-C. (2005) Correlation between microtomography and histomorphometry for assessment of implant osseointegration. *Clinical Oral Implants Research* **16**: 156–160.

Puri, K., Suresh, K., Gogtay, N. & Thatte, U. (2009) Declaration of Helsinki, 2008: implications for stakeholders in research. *Journal of Postgraduate Medicine* **55**: 131–134.

Scherf, H. & Tilgner, R. (2009) A new high-resolution computed tomography (CT) segmentation method for trabecular bone architectural analysis. *American Journal of Physical Anthropology* **140**: 39–51.

Schmitt, C.M., Doering, H., Schmidt, T., Lutz, R., Neukam, F.W. & Schlegel, K.A. (2013) Histological results after maxillary sinus augmentation with Straumann® BoneCeramic, Bio-Oss®, Puros®, and autologous bone. A randomized controlled clinical trial. *Clinical Oral Implants Research;* **24**: 576–585.

Schortinghuis, J., Ruben, J.L., Meijer, H.J., Bronckers, A.L., Raghoebar, G.M. & Stegenga, B. (2003) Microradiography to evaluate bone growth into a rat mandibular defect. *Archives of Oral Biology* **48**: 155–160.

Soardi, C.M., Spinato, S., Zaffe, D. & Wang, H.-L. (2011) Atrophic maxillary floor augmentation by mineralized human bone allograft in sinuses of different size: an histologic and histomorphometric analysis. *Clinical Oral Implants Research* **22**: 560–566.

Soardi, C.M., Zaffe, D., Motroni, A. & Wang, H-L. (2012) Quantitative comparison of cone beam computed tomography and microradiography in the evaluation of bone density after maxillary sinus augmentation: a preliminary study. *Clinical Implant Dentistry and Related Research* doi: 10.1111/cid 12016 [Epub ahead of print].

Stiller, M., Rack, A., Zabler, S., Goebbels, J., Dalügge, O., Jonscher, S. & Knabe, C. (2009) Quantification of bone tissue regeneration employing β-tricalcium phosphate by three-dimensional non-invasive synchrotron micro-tomography — A comparative examination with histomorphometry. *Bone* **44**: 619–628.

Tamminen, I.S., Isaksson, H., Aula, A.S., Honkanen, E., Jurvelin, J.S. & Kröger, H. (2010) Reproducibility and agreement of micro-CT and histomorphometry in human trabecular bone with different metabolic status. *Journal of Bone and Mineral Metabolism* **29**: 442–448.

Thomsen, J.S., Laib, A., Koller, B., Prohaska, S., Mosekilde, L. & Gowin, W. (2005) Stereological measures of trabecular bone structure: comparison of 3D micro computed tomography with 2D histological sections in human proximal tibial bone biopsies. *Journal of Microscopy* **218**: 171–179.

Trisi, P., Rebaudi, A., Calvari, F. & Lazzara, R.J. (2006) Sinus graft with biogran, autogenous bone, and PRP: a report of three cases with histology and micro-CT. *The International Journal of Periodontics and Restorative Dentistry* **26**: 113–125.

Uchiyama, T., Tanizawa, T., Muramatsu, H., Endo, N., Takahashi, H.E. & Hara, T. (1997) A morphometric comparison of trabecular structure of human ilium between microcomputed tomography and conventional histomorphometry. *Calcified Tissue International* **61**: 493–498.

Wallace, S.S. & Froum, S.J. (2003) Effect of maxillary sinus augmentation on the survival of endosseous dental implants. A systematic review. *Annals of Periodontology* **8**: 328–343.

Yeom, H., Blanchard, S., Kim, S., Zunt, S. & Chu, T.-M.G. (2008) Correlation between micro-computed tomography and histomorphometry for assessment of new bone formation in a calvarial experimental model. *The Journal of Craniofacial Surgery* **19**: 446–452.